Frequent Long-Distance Plant Colonization in the Changing Arctic

Inger Greve Alsos, *et al.*

Science **316**, 1606 (2007);
DOI: 10.1126/science.1139178

Science (print ISSN 0036-8075; online ISSN 1095-9203) is published weekly, except the last week in December, by the American Association for the Advancement of Science, 1200 New York Avenue NW, Washington, DC 20005.

Frequent Long-Distance Plant Colonization in the Changing Arctic

Inger Greve Alsos,[1]*† Pernille Bronken Eidesen,[1] Dorothee Ehrich,[1] Inger Skrede,[1] Kristine Westergaard,[1,2] Gro Hilde Jacobsen,[1] Jon Y. Landvik,[3] Pierre Taberlet,[4] Christian Brochmann[1]

The ability of species to track their ecological niche after climate change is a major source of uncertainty in predicting their future distribution. By analyzing DNA fingerprinting (amplified fragment-length polymorphism) of nine plant species, we show that long-distance colonization of a remote arctic archipelago, Svalbard, has occurred repeatedly and from several source regions. Propagules are likely carried by wind and drifting sea ice. The genetic effect of restricted colonization was strongly correlated with the temperature requirements of the species, indicating that establishment limits distribution more than dispersal. Thus, it may be appropriate to assume unlimited dispersal when predicting long-term range shifts in the Arctic.

Climate warming (*1*) is expected to cause the distribution area of many plant species to shift northward in the Northern Hemisphere (Fig. 1). The composition of future ecosystems will critically depend on the long-distance dispersal capabilities of individual species (*2*–*4*). Because long-distance dispersal is supposed to be rare and stochastic, quantification of it poses a considerable challenge (*5*–*8*). Models that are used to forecast climate change–induced shifts in species distribution commonly assume that dispersal is unlimited (*9*, *10*), although restricted dispersal may prevent species from filling their climatic niche (*11*, *12*). Thus, it is important to determine whether species will be able to track their climatic niche. In this study, we used genetic data to reconstruct past plant colonization patterns in the Arctic. In particular, we determined the frequency of effective long-distance dispersal events, identified the source areas, and assessed whether dispersal ability is more limiting than establishment in a new area.

The Svalbard Archipelago (Fig. 2) is a good model system in which to study long-distance dispersal in the Arctic because of its remote location and geological history. The islands were almost entirely glaciated during the last glacial maximum 20,000 years before the present (yr B.P.) (*13*, *14*). It has been debated whether any of Svalbard's flora survived in local refugia (*15*, *16*). Recently, genetic studies have indicated that colonization occurred after the glacial retreat (*15*, *16*). This is in accord with recent reconstructions (*13*), which suggest an extreme ice cover that excluded glacial survival of most, if not all, species. Paleorecords show a sparse arctic vegetation subsequent to 10,000 yr B.P., and pollen and marine mollusc data indicate that the climate was 1° to 2°C warmer than today from 9500 to 4000 yr B.P. (*17*). This warm period probably facilitated colonization of the most thermophilous species occurring in Svalbard today.

We analyzed 4439 samples from most of the geographic ranges of nine plant species native to the Arctic, representing the major climatic and dispersal adaptations found in the region, for amplified fragment-length polymorphism (AFLP) (Table 1) (*18*). To determine the geographic structure of the genetic variation, we used Bayesian clustering analyses, ordination, and tree-building algorithms. The most likely source regions for the plants from Svalbard were determined with multilocus assignment tests. The genetic effect of restricted colonization was quantified by combining six genetic measures. The minimum number of colonizing propagules was estimated as the smallest possible subsample of the source populations needed to bring all observed AFLP markers to Svalbard (*18*).

We found that colonization of Svalbard has occurred from all possible adjacent source regions (Fig. 2), suggesting that future colonization from the same regions can be expected. We observed a variety of species-specific patterns, as typically found in comparative phylogeography (*19*). Notably, the predominant source was the most distant region, northwestern Russia. Colonization from Scandinavia was rare; only *Salix herbacea* appears to have derived mainly from this region (Fig. 2). However, the single Russian population of *S. herbacea* that we analyzed belonged to the same genetic group as the northern Scandinavian populations, and colonization from the east could not be excluded even for this species.

In eight of the nine species, multiple propagules were necessary to bring the observed genetic diversity to Svalbard (Table 1; *Arabis alpina* was virtually invariable in the North Atlantic region). We estimated that a minimum number of 6 to 38 plants of each species must have successfully established and survived in Svalbard, implying that many more propagules actually reached the archipelago (*18*). In addition to the main source region, the allocation tests (Fig. 2) and the geographic distribution of the AFLP markers (not shown) indicated supplementary source regions for six species. The most hardy species, which are adapted to mean July temperatures of 4° to 5°C or colder (*Dryas octopetala*, *Salix herbacea*, *Cassiope tetragona*, and *Saxifraga rivularis*), were allocated to several source regions and had the highest estimates of colonizing propagules. In these species, the level of genetic diversity in Svalbard was similar to that in the primary source regions (Table 1). More than one source

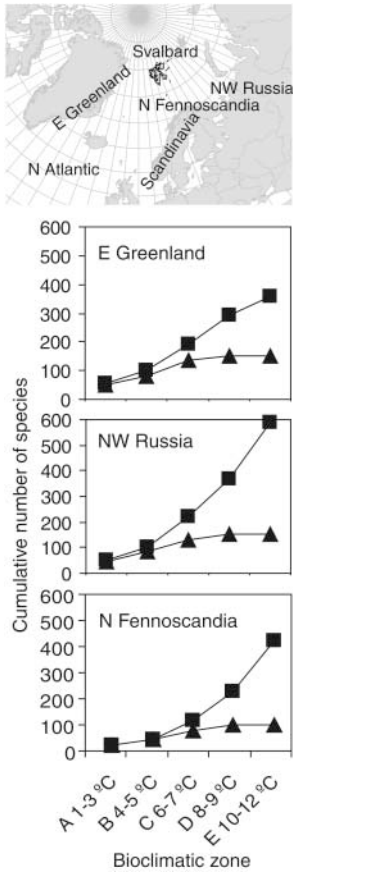

Fig. 1. Number of species that may colonize the geographically isolated Svalbard archipelago (map) from adjacent land masses after climate warming. The graphs show cumulative number of species in successively warmer bioclimatic zones in the source regions (squares) and the cumulative number of these species that are present in Svalbard today (triangles) (*18*). Mean July temperature is given for each bioclimatic zone. Most of Svalbard's current flora belong to zones A to C. A summer temperature increase of 2° to 4°C (*1*) could shift Svalbard toward zones D and E. The gap between the lines at bioclimatic zone D and E shows high potential numbers of colonizing species.

[1]National Centre for Biosystematics, Natural History Museum, University of Oslo, Post Office Box 1172 Blindern, NO-0318 Oslo, Norway. [2]Tromsø University Museum, University of Tromsø, NO-9037 Tromsø, Norway. [3]Norwegian University of Life Sciences, Post Office Box 5003, NO-1432 Ås, Norway. [4]Laboratoire d'Ecologie Alpine, CNRS UMR 5553, Université Joseph Fourier, Post Office Box 53, F-38041 Grenoble Cedex 09, France.

*To whom correspondence should be addressed. E-mail: ingera@unis.no

†Present address: The University Centre in Svalbard, Post Office Box 156, NO-9171 Svalbard, Norway.

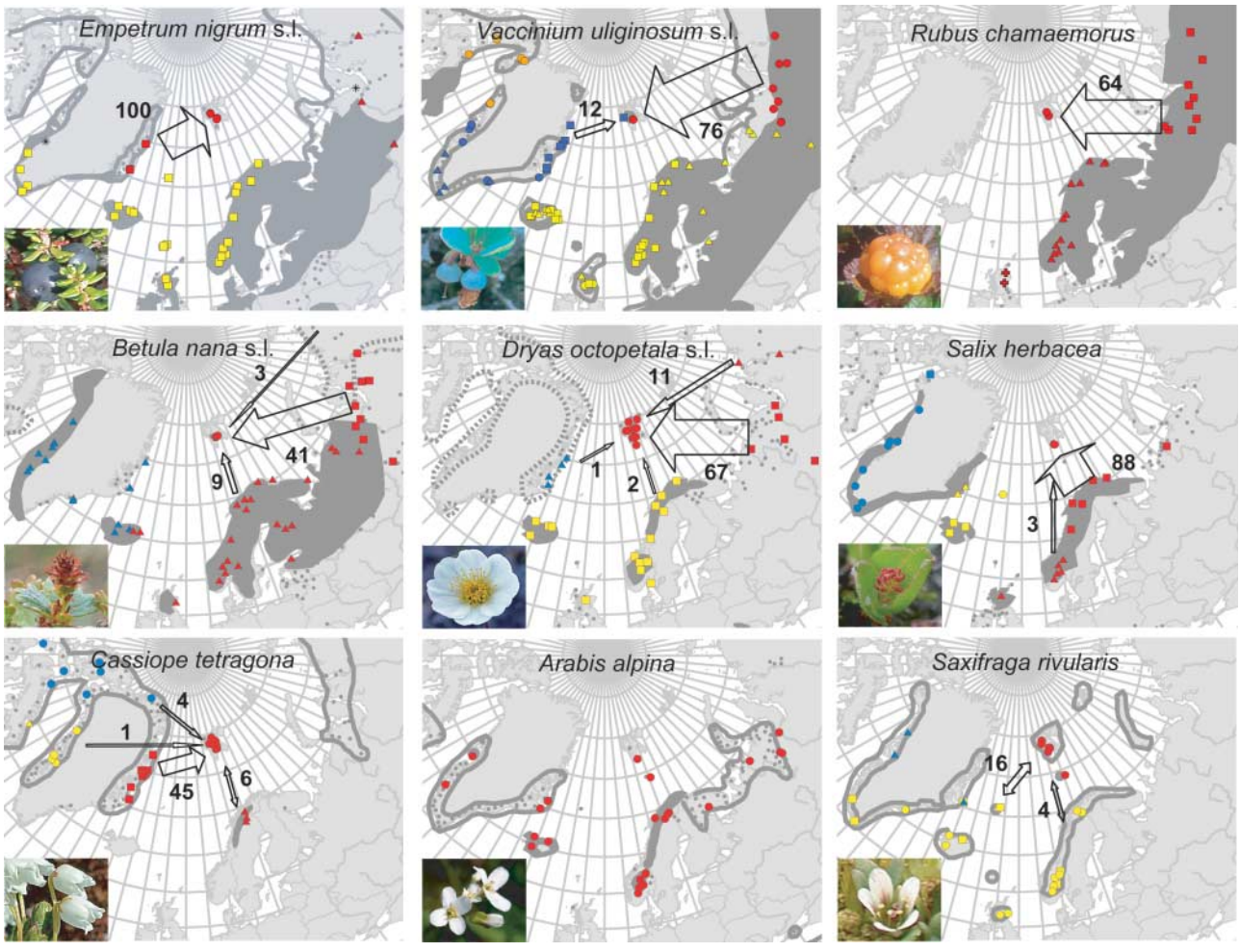

Fig. 2. Source regions for past colonization of Svalbard inferred from genetic data (AFLP). The geographic distribution of the species (*23*, *24*) is shaded, and the distribution of closely related species is indicated by dotted lines (*Betula exilis* and *Dryas integrifolia*). Colors represent main genetic groups and symbols represent subgroups. Asterisks indicate a population that could not be clearly placed into a genetic group (*E. nigrum*). Numbers on the arrows indicate the percentage allocation when a log-likelihood difference of 1 was used (10 times as likely from that source region as from any other source regions). For *C. tetragona*, the direction of dispersal between Svalbard and Scandinavia is uncertain because of low diversity in Scandinavia. The source for the Svalbard populations of *A. alpina* could not be determined because of lack of genetic variation. In *S. rivularis*, the highest levels of genetic variation and most private markers were observed in the Svalbard populations (Table 1), which also were clearly separated from the two amphi-Atlantic genetic groups. Thus, survival in Svalbard during the last glacial maximum cannot be excluded for this high-arctic species.

region was also found in two of the rarest and most thermophilous species in Svalbard, *Betula nana* and *Vaccinium uliginosum*.

The genetic effect of restricted colonization of Svalbard was negatively correlated with adaptation to the current climate in Svalbard (Fig. 3), suggesting that dispersal itself may not be the limiting factor. The establishment phase—involving germination, survival, and local reproduction—is more likely to be the limiting process. This interpretation is supported by our observation that 80 to 90% of the most cold-adapted species that occur in the potential source regions are currently present in Svalbard, whereas only 40 to 60% of the species limited to bioclimatic zone C (6° to 7° C July temperature) are present in Svalbard (Fig. 1).

Probable dispersal vectors are wind (which may have carried propagules through the air or over snow and sea ice), drift wood and drifting sea ice, birds, and mammals (*3*, *5*, *8*, *20*, *21*). In contrast to Scandinavia, northwestern Russia and Greenland are frequently connected to Svalbard by way of sea ice during winter. Dispersal from Russia may have been facilitated by drift wood. Bank erosion along the Russian rivers routinely results in logs and other debris finding their way onto drifting sea ice, which reaches Svalbard by means of surface currents (*20*).

The recurrent glacial cycles have probably selected for a highly mobile arctic flora. In addition, some dispersal vectors may be particularly efficient in the Arctic as a result of the open landscape, strong winds, and extensive snow and ice cover. The high levels of genetic diversity found in several species previously studied in Svalbard are also consistent with multiple dispersals, although the sampling design and genetic methods used did not allow estimation of the frequency or source areas (*16*, *22*). Given that

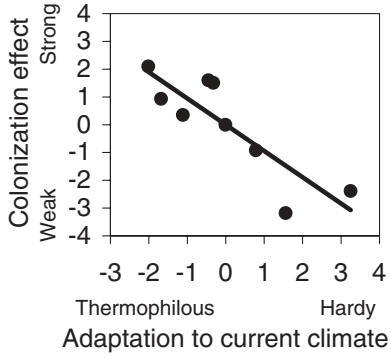

Fig. 3. Index of the genetic effect of restricted colonization of Svalbard for the nine species analyzed compared with an index of adaptation to the current climate in Svalbard. The axes are principal components summarizing three measures of climatic adaptations (Table 1) and six quantities related to the effect of restricted colonization based on genetic data (AFLP) (*18*).

Table 1. Characteristics of the species analyzed and AFLP data. The northernmost bioclimatic zone where the species is frequent (f) or scattered (s) is given according to the checklist in Elven *et al*. (*24*). B, Northern Arctic tundra zone; C, Middle Arctic tundra zone; D, Southern Arctic tundra zone. The relative rarity—i.e., how much rarer the species is in Svalbard compared with the abundance reached in its optimal habitat—is based on our own observations (1 = rare and 6 = abundant). The minimum number of propagules that colonized Svalbard, genetic diversity (*D*) (± standard deviation), and differentiation (Φ_{ST}) within Svalbard and between Svalbard, and the most important source region (compare with Fig. 2) are calculated based on the AFLP data. For *S. rivularis*, two data sets were analyzed (*18*).

	Empetrum nigrum L. s.l.	*Vaccinium uliginosum* L. s.l.	*Rubus chamaemorus* L.	*Betula nana* L. s.l.	*Dryas octopetala* L. s.l.	*Salix herbacea* L.	*Cassiope tetragona* (L.) D. Don ssp. *tetragona*	*Arabis alpina* L.	*Saxifraga rivularis* L.
Main dispersal vector	Bird	Bird	Bird	Wind	Wind	Wind	Wind?	Wind?	Wind?
Northernmost bioclimatic zone	C (s)	C (s)	D (f)	D (f)	C (f)	C (s)	C (f)	C (f)	B (f)
Minimum mean July temperature (°C) (*25*)	5 to 6	5 to 6	6 to 7?	6 to 7	3 to 4	4 to 5	4 to 5	5 to 6	<3
Relative rarity in Svalbard	3	1	1	2	5	3	4	2	6
Germinable seeds or seed banks in Svalbard (*26*)	No data	Not found	No data	Not found	Only in warmest sites	No data	Rare	No data	Abundant
No. of populations analyzed (Svalbard)	46 (4)	131 (3)	45 (2)	71 (5)	72 (21)	41 (3)	58 (12)	36 (2)	32/22 (8)
No. of individuals analyzed (Svalbard individuals/ genets)	435 (38/32)	957 (26/17)	398 (15/14)	570 (32/29)	528 (161)	399 (33/32)	579 (132)	305 (10)	268/207(72)
No. of polymorphic markers (private Svalbard)	78 (0)	105 (0)	173 (0)	119 (1)	155 (1)	250 (1)	171 (1)	242 (0)	45 (2) / 78 (8)
AFLP reproducibility % (no. of controls)	97.7 (30)	97.7 (44)	97.8 (63)	98.0 (51)	99.1 (32)	98.0 (41)	99.3 (23)	99.0 (42)	97.3 (104) / 95.0 (40)
Minimum no. of colonizing propagules	7	12	6	11	38	20	14	1	22
D Svalbard (average per population)	0.049 ± 0.017	0.066 ± 0.044	0.060 ± 0.019	0.103 ± 0.016	0.089 ± 0.025	0.104 ± 0.007	0.125 ± 0.010	0.000	0.122 ± 0.074
D main source region (average per population)	0.118 ± 0.032	0.174 ± 0.020	0.126 ± 0.011	0.148 ± 0.013	0.106 ± 0.017	0.142 ± 0.015	0.133 ± 0.011	0.001 ± 0.002	0.061 ± 0.024
Φ_{ST} within Svalbard	0.275	0.696	0.272	0.161	0.151	0.188	0.167	–	0.483
Φ_{ST} Svalbard—main source region	0.147	0.049	0.109	0.113	0.157	0.110	0.013	0.000	0.211

the dispersal mechanisms in existence during the early and mid-Holocene are probably still operating today, we can assume that long-distance dispersal still occurs with regularity. Thus, we concluded that arctic species seem to be able to track their potential niche and that unlimited dispersal models (*9*, *10*) may be appropriate to estimate long-term range shifts for arctic regions.

References and Notes

1. ACIA, *Arctic Climate Impact Assessment: Scientific Report* (Cambridge Univ. Press, Cambridge, 2006).
2. M. L. Cain, B. G. Milligan, A. E. Strand, *Am. J. Bot.* **87**, 1217 (2000).
3. S. I. Higgins, R. Nathan, M. L. Cain, *Ecology* **84**, 1945 (2003).
4. T. V. Callaghan *et al.*, *Ambio* **33**, 404 (2004).
5. R. Nathan, *Science* **313**, 786 (2006).
6. R. Nathan, G. Perry, J. T. Cronin, A. E. Strand, M. L. Cain, *Oikos* **103**, 261 (2003).
7. S. I. Higgins *et al.*, *J. Ecol.* **91**, 341 (2003).
8. R. P. Neilson *et al.*, *Bioscience* **55**, 749 (2005).
9. W. Thuiller, S. Lavorel, M. B. Araujo, M. T. Sykes, I. C. Prentice, *Proc. Natl. Acad. Sci. U.S.A.* **102**, 8245 (2005).
10. A. Guisan, W. Thuiller, *Ecol. Lett.* **8**, 993 (2005).
11. J.-C. Svenning, F. Skov, *Ecol. Lett.* **7**, 565 (2004).
12. K. A. Moore, S. C. Elmendorf, *Ecol. Lett.* **9**, 797 (2006).
13. J. Y. Landvik *et al.*, *Quat. Sci. Rev.* **17**, 43 (1998).
14. J. Y. Landvik *et al.*, *Geology* **31**, 905 (2003).
15. O. I. Rønning, in *North Atlantic Biota and Their History*, Á. Löve, D. Löve, Eds. (Pergamon Press, Oxford, 1963), pp. 99–107.
16. C. Brochmann, T. M. Gabrielsen, I. Nordal, J. Y. Landvik, R. Elven, *Taxon* **52**, 417 (2003).
17. H. H. Birks *et al.*, *J. Quat. Sci.* **9**, 133 (1994).
18. Materials and methods are available as supporting material on *Science* Online.
19. P. Taberlet, L. Fumagalli, A. G. Wust-Saucy, J. F. Cosson, *Mol. Ecol.* **7**, 453 (1998).
20. S. Johansen, H. Hytteborn, *J. Biogeogr.* **28**, 105 (2001).
21. R. Nathan *et al.*, *Nature* **418**, 409 (2002).
22. R. J. Abbott *et al.*, *Science* **289**, 1343 (2000).
23. E. Hultén, M. Fries, *Atlas of North European Vascular Plants North of the Tropic of Cancer* (Koeltz Scientific Books, Königstein, Germany, 1986).
24. R. Elven, D. F. Murray, V. Razzhivin, B. A. Yurtsev, *Checklist of the Panarctic Flora (PAF): Vascular Plants* (Univ. of Oslo, Oslo, Norway, 2005).
25. S. R. Karlsen, A. Elvebakk, *J. Biogeogr.* **30**, 1469 (2003).
26. E. J. Cooper *et al.*, *J. Veg. Sci.* **15**, 115 (2004).

27. We thank our many colleagues and field assistants (table S1) for help with providing plant samples; the authorities in various regions for collection permits and help with field logistics; L. G. Kvernstuen for laboratory assistance; B. E. Sandbakk for photographs; A. Tribsch, P. Schönswetter, R. Elven, and L. Bachmann for discussions; and W. Thuiller, I. Till-Bottraud, K. Kovacs, and three anonymous referees for valuable comments on the manuscript. Part of the material was obtained by means of the Tundra North-West (TNW) 1999 and the

Beringia 2005 expeditions funded by the Polar Research Secretariat at the Royal Swedish Academy of Sciences. The main work was funded by grant 150322/720 to Brochmann from the Research Council of Norway. Additional grants to Westergaard were obtained from K. and H. Jakobsens Fund, King Haakon VII Educational Fund, Roald Amundsen's Centre for Arctic Research, KOMETEN, and Tromsø University Museum.

Supporting Online Material

www.sciencemag.org/cgi/content/full/316/5831/1606/DC1
Materials and Methods
Tables S1 and S2
References

22 December 2006; accepted 2 May 2007
10.1126/science.1139178

Modulation of Neuronal Interactions Through Neuronal Synchronization

Thilo Womelsdorf,[1]*† Jan-Mathijs Schoffelen,[1]*† Robert Oostenveld,[1] Wolf Singer,[2,3] Robert Desimone,[4,5] Andreas K. Engel,[6] Pascal Fries[1,7]

Brain processing depends on the interactions between neuronal groups. Those interactions are governed by the pattern of anatomical connections and by yet unknown mechanisms that modulate the effective strength of a given connection. We found that the mutual influence among neuronal groups depends on the phase relation between rhythmic activities within the groups. Phase relations supporting interactions between the groups preceded those interactions by a few milliseconds, consistent with a mechanistic role. These effects were specific in time, frequency, and space, and we therefore propose that the pattern of synchronization flexibly determines the pattern of neuronal interactions.

Groups of activated neurons synchronize in the gamma-frequency band (30 to 100 Hz), and previous studies have related gamma-band synchronization to several cognitive functions (*1*–*6*). Yet, if gamma-band synchronization subserves those functions, it must have mechanistic consequences for neuronal processing (*7*). It has been shown that the precise timing of pre- and postsynaptic activation determines long-term changes in synaptic strength (*8*–*10*) and that gamma-band synchronization of synaptic inputs directly enhances their effective synaptic strength (*11*–*13*).

Synchronization between two groups of neurons is also likely to facilitate interactions between them (Fig. 1A) (*6*, *14*). Gamma-band synchronization entails rhythmic inhibition of the local network (*15*–*17*), and the periods between inhibition provide temporal windows for neuronal interaction. Two groups of neurons will therefore probably have a greater influence on each other when their temporal interaction windows open at the same times, i.e., when the rhythmic synchronization within the groups is also synchronized between the groups. By the same token, the interaction is probably curtailed if the temporal interaction windows open either in an uncorrelated way or consistently out of phase with each other.

We analyzed four data sets: (i) one from awake cat area 17, (ii) one combining awake cat area 18 with area 21a recordings, (iii) one from awake monkey area V1, and (iv) one from monkey area V4. [Data from two of the three area 17 data sets have been used in (*18*, *19*); the V4 data set has been used in (*3*, *20*).] In all cases, we recorded multiunit activity (MUA) and local field potentials (LFPs) simultaneously from four to eight electrodes while the neurons were visually stimulated with moving gratings. From each data set, we used trials with identical visual stimulation and behavioral tasks and based our analysis on the natural fluctuation of neuronal gamma-band synchronization. For each pair of neuronal groups, we quantified synchronization by means of the MUA-MUA phase-coherence spectrum (Fig. 1B) and the MUA-LFP phase-coherence spectrum (Fig. 1C) (*21*).

Phase-coherence spectra showed a peak in the gamma-frequency band, indicating that phase relations between signals were not random. However, phase coherence was far from perfect (a value of 1.0), but it assumed average peak values of 0.14 and 0.27 for MUA-MUA and MUA-LFP combinations, respectively. The phase relations at 60 Hz in one example MUA-MUA pair are shown for 708 trials of 250-ms length (phase-coherence value of 0.06) (Fig. 1D).

The spread of phase relations around their mean might just be irrelevant noise. Here, however, we used this spread to actually test for its potential physiological consequences. We hypothesized that the mutual influence between two neuronal groups was a function of their phase relation (Fig. 1A). Phase relations are meaningfully defined per frequency, and we hypothesized that the phase relation at a given frequency should modulate the interaction among the local rhythmic activities specifically at that frequency.

We investigated this hypothesis for the example pair of recordings sites. We sorted the trials into six bins according to the 60-Hz phase relation between the two MUAs (Fig. 1D). For each phase-relation bin separately, we then quantified the two MUAs' mutual influence as the Spearman rank correlation coefficient between the two MUAs' 60-Hz power, across the trials in the bin (Fig. 1E). Fluctuations of 60-Hz power were most strongly correlated when the 60-Hz phase relation was close to its mean across the trials. Specifically, when the gamma-band rhythm in group A led the one in group B by 2.1 ms (mean phase relation at 45.8°), the correlation between each group's gamma-band power was four times as strong as when the rhythms were separated by 10.5 ms (phase relation at 225.8°). The example pair illustrates this for a case with a nonzero mean phase to demonstrate that the effect cannot be ascribed to external artifacts or volume conduction, but the mean phase relations across our sample distributed closely around zero (Fig. 1B).

We performed the same analysis after replacing one of the MUAs by the LFP recorded through the same electrode. The mean MUA-LFP phase relations clustered around 141° (Fig. 1C), and power correlations were again substantially enhanced around the mean phase relation (Fig. 1, F and G). Across our sample, good phase relations mostly distributed close to the respective mean phase relations for both MUA-MUA and MUA-LFP pairs (fig. S1). We correspondingly dubbed the mean phase relation as "good" and the opposite phase relation as "bad," and we aligned the trial binning to the good phase relation.

The observed effect was consistent across the four data sets (Fig. 2 and fig. S2) (140, 86, 111, and 111 MUA-MUA pairs from area 17, areas 18×21a, area V1, and area V4, respectively, and 280, 172, 228, and 237 MUA-LFP pairs from the same areas). MUA-LFP pairs showed qualitatively the same effect as MUA-MUA pairs but with higher signal-to-noise ratios (Fig. 2B). We therefore focused our further analyses on MUA-LFP pairs (recorded from separate electrodes). The effect was also present for pairs of LFP and single-unit recordings (fig. S3). The effect generalized to long-range interactions, because the analysis of the data set combining cat area

[1]F. C. Donders Centre for Cognitive Neuroimaging, Radboud University Nijmegen, 6525 EN Nijmegen, Netherlands. [2]Department of Neurophysiology, Max Planck Institute for Brain Research, 60528 Frankfurt, Germany. [3]Frankfurt Institute for Advanced Studies, Johann Wolfgang Goethe University, 60438 Frankfurt, Germany. [4]Laboratory of Neuropsychology, National Institute of Mental Health, National Institutes of Health, Bethesda, MD 20892, USA. [5]McGovern Institute for Brain Research, Massachusetts Institute of Technology, Cambridge, MA 02139, USA. [6]Department of Neurophysiology and Pathophysiology, University Medical Center Hamburg-Eppendorf, 20246 Hamburg, Germany. [7]Department of Biophysics, Radboud University Nijmegen, 6525 EZ Nijmegen, Netherlands.

*These authors contributed equally to this work.
†To whom correspondence should be addressed. E-mail: thilo.womelsdorf@fcdonders.ru.nl (T.W.); jan.schoffelen@fcdonders.ru.nl (J.-M.S.)